Electronic Supplementary Material (ESI) for RSC Advances.

Synthesis of reduced graphene oxide-montmorillonite nanocomposite and its application in hexavalent chromium removal from aqueous solutions

Zilong Zhang[†, ‡], Hanjin Luo[†, ‡,*], Xiaolu Jiang[†, ‡], Chen Yang[†, ‡], Zhongjie Jiang[†]

[†] School of Environment and Energy, South China University of Technology, Guangzhou Higher Education Mega Centre, Guangzhou 510006, PR China

[‡] The Key Lab of Pollution Control and Ecosystem Restoration in Industry Clusters, Ministry of Education, South China University of Technology, Guangzhou Higher Education Mega Centre, Guangzhou 510006, PR China

Tel: 0086-20-87110517

Fax: 0086-20-39380508

E-mail: luohj@scut.edu.cn

S1. Preparation of GO and CM suspension

GO was prepared from natural graphite powder via a modified Hummers method. In brief, 5 g graphite and 2.5 g $NaNO_3$ were added into 120 ml of concentrated H_2SO_4 solution. The mixture was stirred constantly for 0.5 h with an electric mixer in ice bath. 15 g $KMnO_4$ was then added slowly under vigorous stirring, with the temperature kept below 5 ºC via ice bath. After 1.5 h, the mixture was moved from ice bath to water bath at 35 ºC, and stirred for another 0.5 h. 230 ml of deionized water was then added dropwise, which led to a rapid increase of the temperature to 95 ºC. After 0.5 h, 50 ml of H_2O_2 (30%) solution was added. The resulting material was vacuum filtered and washed with HCl (5%) solution several times, followed by washing copiously with deionized water until to pH=7.0. The gel-like GO was vacuum-dried at 60 ºC for 3 days.

The organic modified montmorillonite (CM) was synthesized by solvent method. Firstly, the cetyltrimethylammonium bromide (CTAB) solution was prepared by dissolving CTAB in deionized water in a 100 ml beaker. The amount of CTAB used was 125% of CEC. Secondly, 2.5 g raw Mt was added into the CTAB solution under agitation. The reaction was conducted in water bath at 60 ºC. After 2.0 h of stirring, the mixture was collected through vacuum filtration and washed with deionized water several times until no precipitation was observed when detected with 0.1 mol L^{-1} $AgNO_3$ solution. The obtained product was re-dispersed in 50 ml deionized water to form CM suspension.

S2. Methods of characterization

Powder X-ray diffractograms (PXRD) of the samples were obtained using a Bruker D8 Advance X-ray diffractometer (Bruker, Germany) at 40 kV and 40 mA, whereas the 2θ angles ranged between 2º and 60º with a step scanning speed of 0.020º /step and 17.7 s/step. A Cu Kα radiation source (λ=1.5418 Å) was employed in the PXRD test. Fourier transform infrared spectra (FT-IR) patterns of the samples were determined using a Tensor 27 spectrophotometer (Bruker, Gernany). The FT-IR spectra in the range of 4000~400 cm^{-1} were recorded at a resolution of 4 cm^{-1}. The powdered samples were blended with KBr (FT-IR grade, Aladdin Industrial Co., Ltd, Shanghai, China) with an agate mortar and pressed into tablet prior to test. The morphology of GCM nanocomposites was determined by using a JEM 2100F transmission electron microscope (TEM) (JEOL, Japan) with accelerating voltage of 200 kV. The powdered specimens were dispersed in absolute ethanol by ultrasonication for 30 minutes before placed on 230-mesh copper grids coated with carbon film (Zhongjingkeyi Technology Co., Ltd., Guangzhou, China). The surface area of the samples were determined by the method of Brunauer-Emmett-Teller (BET) with a surface area and porosity analyzer (ASAP 2020, Micromeritics, USA). All the samples were degassed for 12 hours at 60 ºC under vacuum. The surface area was determined with nitrogen adsorption/desorption technique at −198 ºC. X-ray fluorescence (XRF) was employed to estimate the quantity of elemental oxides exist in raw montmorillonite and GCM with an Axios PW4400 Wavelength Dispersive X-Ray Fluorescence Spectrometer (PANalytical, Netherlands). Thermogravimetric analysis (TGA) was performed at a SDT-Q600 thermogravimetric analyzer (TA

Instruments-Waters LLC, USA) from 30 ºC to 1000 ºC at a heating rate of 10 ºC min^{-1} under nitrogen atmosphere with a nitrogen flow rate of 100 ml min^{-1}. The mass of the samples were recorded as a function of temperature.

S3. Component analysis

The chemical compositions of the samples were measured by X-ray fluorescence (XRF) spectrometry, with the results shown in Table 1. The loss on ignition (LOI) can be used to estimate the approximate amount of organic matter, i.e., CTAB and/or rGO in raw and modified Mt. The LOIs of CM and GCM nanocomposites were significantly greater relative to raw Mt, indicating the intercalation of CTA$^+$ in Mt and hybridization between rGO and CM, which is consistent with the analysis of XRD and TEM. The raw Mt consisted mainly of SiO_2 and Al_2O_3 (up to 85 wt. %) with a small contribution from other oxides according to the XRF data. The data in Table 1 show that CaO practically disappeared from the GCM, which is initially detected in Mt, confirming that Ca^{2+} was the dominant exchangeable cation present in the interlayer space, easily exchanging with CTA$^+$ cations during the organic modification process.

Table S1. Chemical compositions (wt. %) of the natural and modified materials.

	Mt	CM	GCM10	GCM20	GCM30
Loss on ignition	—	13.88	18.78	25.11	25.23
MgO	3.78	3.32	2.87	2.86	2.82
Al_2O_3	13.09	11.56	12.62	10.50	11.94
SiO_2	75.79	67.13	61.88	57.52	56.01
SO3	0.21	0.15	0.26	0.26	0.23
K_2O	0.09	0.09	0.03	0.10	0.13
TiO_2	0.28	0.19	0.27	0.22	0.27

Fe_2O_3	4.14	3.45	3.10	3.16	2.87
NiO	—	0.06	0.10	0.15	0.13
ZrO_2	0.12	0.10	0.09	0.08	0.06
ZnO	—	—	—	0.05	—
Cl	—	—	—	—	0.31
CaO	2.48	—	—	—	—
SrO	0.02	—	—	—	—

S4. Brunauer-Emmett-Teller (BET) analysis

The Multi-Point BET Plots of Mt, CM and GCM20 are shown in Fig. S1.

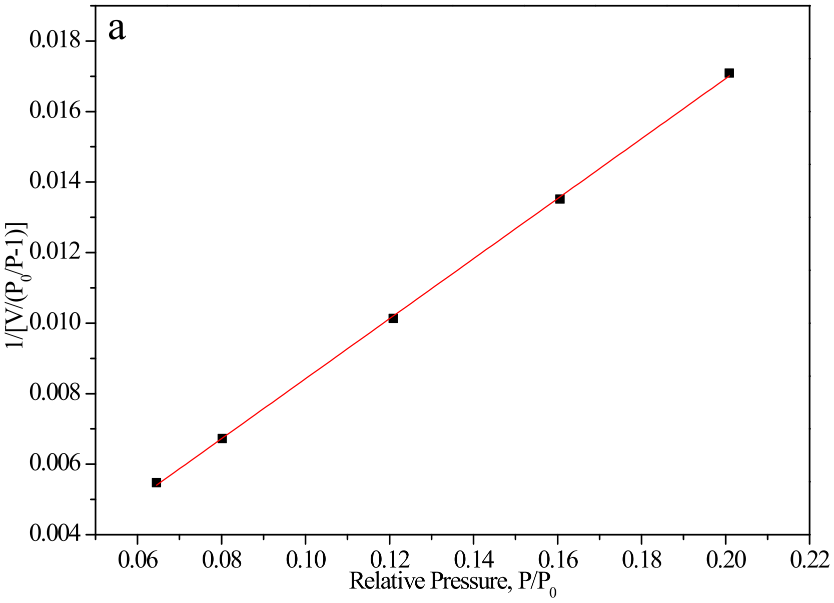

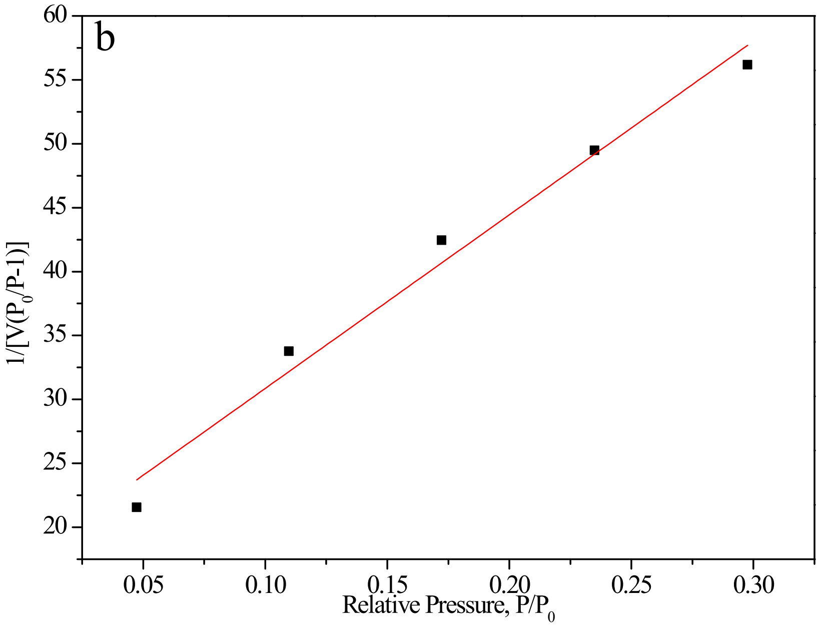

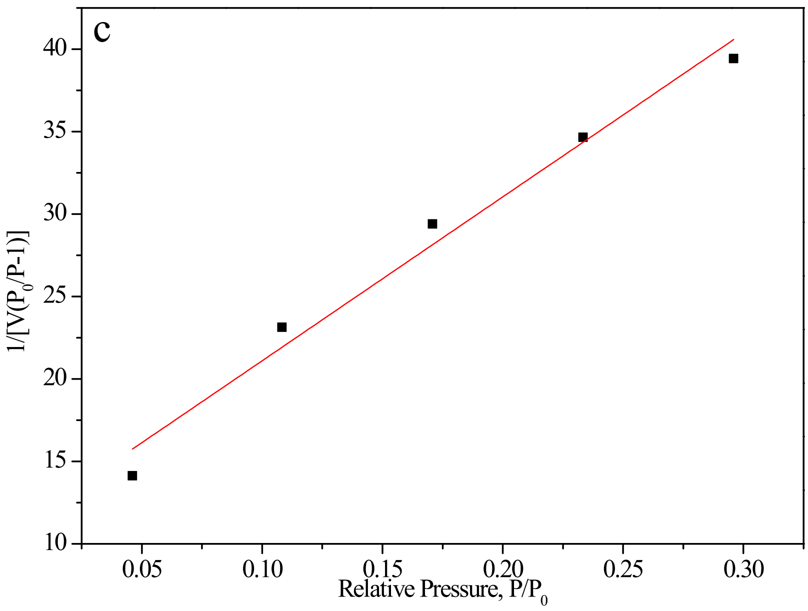

Fig. S1 The Multi-Point BET Plots of a) Mt, b) CM and c) GCM20

S4. Cr (VI) adsorption experiments

The initial pH on adsorption varied a range of 2.0~12.0 by agitating adsorbents (0.15 g) with Cr (VI) solution (50 ppm, 25 ml) for 120 min at 25±0.2 ºC. The pH was adjusted using a calibrated PHS-3C pH meter (Shanghai), as needed, with additions of 0.1 mol L^{-1} HCl and/or NaOH.

For the kinetic experiments, the adsorbents (0.15 g) were placed in a series of stoppered 50-ml conical flasks containing 25 ml Cr (VI) solution (50 and 100 ppm, pH 2.0). The flasks were put into a thermostated shaker and stirred for suitable time intervals at 25±0.2 ºC.

Adsorption of Cr (VI) was also studied at 25±0.2 ºC with the dosages of adsorbents varying from 2 g L^{-1} to 20 g L^{-1}, using Cr (VI) solutions of concentration of 50 ppm and 100 ppm at pH 2.0 which were allowed to equilibrate with the adsorbents for 120 min.

Isothermal studies were conducted at different temperatures (20 ºC and 30 ºC) by agitating adsorbents (0.15 g) with 25 ml Cr (VI) solution of varying concentrations from 15 to 90 ppm for 120 min.

All the experiments were conducted in triplicate at a fixed temperature in a thermostated shaker with a rotational speed of 180 rpm. In all cases, after removal from the shaker, the mixtures were allowed to let stand for 5 min before being filtered through a 0.45 μm filter membrane. The filtrates were stored in pre-cleaned glass bottles. The filtrates were used for the quantification of residual concentration of Cr (VI) in the solution.

S5. Recyclability experiments

Adsorption-desorption experiments were carried out by using NaOH solutions of varying concentrations and volumes as the eluant. Before desorption experiments, GCM20 was first equilibrated with Cr (VI) to obtain the maximum loading of chromium. To this end, 0.15 g GCM20 was added to 25 ml Cr (VI) solution (50 ppm, pH 2.0) and the mixture was stirred at 25 ºC and 180 rpm for 120 min. After adsorption equilibration, the suspension was allowed to settle until the supernatant was clear. Then, a small part of the supernatant was filtered and stored for the determination of adsorptive capacity of Cr (VI) on GCM20, while the excess supernatant was discarded and the Cr (VI)-loaded adsorbent was washed with deionized water and separated by centrifugation three times.

The influence of the concentration of NaOH solution on the extent of desorption was studied by adding the Cr (VI)-loaded adsorbent (0.15 g, dry weight) into 25 ml NaOH solution of varying concentrations from 10^{-6} to 1 mol L^{-1} and stirring for 90 min. The impact of the volume of NaOH solution on desorption was investigated by shaking Cr (VI)-loaded adsorbent (0.15 g, dry weight) with 0.1 mol L^{-1} NaOH solution of varying volumes from 10 to 90 ml and stirring for 90 min. The desorption experiments were also studied with different contact time by shaking Cr (VI)-loaded adsorbent (0.15 g, dry weight) with NaOH solution (0.1 mol L^{-1}, 20 ml) for a predetermined time intervals. In all cases, the mixtures were stirred in a thermostated shaker with a rotational speed of 180 rpm and at temperature of 30 ºC. After desorption, the suspension was filtered through a 0.45μm filter membrane and stored for the determination of desorption extent of Cr (VI).

After the desorption process described above under the condition of optimal concentration and volume (0.1 mol L^{-1}, 20 ml) of NaOH solution and contact time (90 min), the adsorbent was washed thoroughly with deionized water, and air-dried at 50 ºC before being grounded and passed through a 200-mesh sieve. The powdered adsorbent was used in the subsequent adsorption-desorption experiments. Six cycles of adsorption-desorption processes were performed.

S6. Adsorption dynamics analysis

The pseudo-first-order kinetic model can be expressed by the following Lagergren rate expression:

$$\log\ (q_e - q_t) = log\ q_e - \frac{k_1 t}{2.303}$$

(1)

where q_e (mg g^{-1}) and q_t (mg g^{-1}) are the amounts of sorbate adsorbed at equilibrium and at contact time t (min), respectively, and k_1 (min^{-1}) is the adsorption rate constant of pseudo-first-order adsorption. The values of q_e and k_1 for the pseudo-first-order model were calculated from the intercept and slope of the plot of log (q_e—q_t) versus t, respectively.

The pseudo-second-order kinetic model can be described by the following expression:

$$\frac{t}{q_t} = \frac{t}{q_e} + \frac{1}{k_2 q_e^2}$$

(2)

where k_2 (g mg^{-1} min^{-1}) is the rate constant of pseudo-second-order adsorption, q_e (mg g^{-1}) and q_t (mg g^{-1}) represent the adsorbed amounts of sorbate at equilibrium and at contact time t (min), respectively. The k_2 and q_e values are determined from the intercept and slope of the plot of t/q_t versus t, respectively.

In general, the rate of adsorption depends on the rate determining step, which is usually either external film or intraparticle diffusion. In order to substantiate the potential rate-determining step and further study the diffusion mechanism, the Weber-Morris intraparticle diffusion model was employed to analyze the experimental data:

$$q_t = k_{pi} t^{1/2} + c_i \tag{3}$$

where q_t (mg g^{-1}) is the amount of sorbate adsorbed at time t (min), k_{pi} is the intraparticle diffusion rate constant (mg g^{-1} min$^{-1/2}$) at stage i and c_i is the intercept corresponding to stage i, which is proportional to the boundary layer thickness. The values of k_{pi} and c_i can be evaluated from the linear plots of q_t versus $t^{1/2}$.

S7. Adsorption isotherms analysis

Langmuir isotherm model, which is based on the assumption that adsorption takes place on homogeneous surface, is a well-studied monolayer adsorption model in various adsorption systems. The linear equation of the Langmuir model is:

$$\frac{c_e}{q_e} = \frac{c_e}{q_m} + \frac{1}{k_L q_m} \quad (4)$$

where c_e (mg L^{-1}) and q_e (mg g^{-1}) are the equilibrium concentration of sorbate in the solution and the amount of adsorbed sorbate per unit weight of sorbent respectively, q_m is the monolayer adsorptive capacity (mg g^{-1}); and k_L (L mg^{-1}) is the Langmuir constant related to free energy of adsorption. The value of q_m and k_L can be obtained from the slop and intercept of the plot of c_e/q_e against c_e, respectively. Furthermore, essential characteristic of a Langmuir model can be expressed in term of a dimensionless constant separation factor (R_L) [1], which is defined by the following equation:

$$R_L = \frac{1}{1 + k_L c_0}$$

(5)

where k_L (L mg^{-1}) is the Langmuir constant; c_0 (mg L^{-1}) is the highest initial sorbate concentration in the solution. According to the value of R_L, one can identify the types of equilibrium isotherm, such as unfavorable (R_L>1), linear (R_L=1), favorable (0<R_L<1), and irreversible (R_L=0).

The Freundlich isotherm model is more general than the Langmuir model, because it is an empirical equation and does not assume a homogenous surface or constant sorption potential. The model is usually expressed as the following linear expression:

$$\ln q_e = \frac{1}{n} \ln c_e + \ln k_F \quad (6)$$

where q_e (mg g^{-1}) is the amount of solute adsorbed per unit mass of sorbent, c_e (mg L^{-1}) is the equilibrium concentration of solute in the solution, k_F (mg g^{-1}) is the Freundlich constant indicative of the adsorptive capacity of the sorbent, and 1/n is a constant indicative of the intensity of the adsorption. The constants k_F and 1/n are evaluated from the intercept and slope of the plot of ln q_e versus ln c_e.

Table S2. Comparison of the adsorption conditions and adsorption capacities.

Adsorbents	pH	Temp (°C)	Adsorption capacity (mg g^{-1})	Ref.
Fe^0/Fe_2O_3/Si-S-O-GNs	7.0	25	1.0	2
ED-RGO	2.0	33	5.0	3
GNs	4.25	20	43	4
Amino starch	3.5	30	12.12	5
Hexadecylpyridinium bromide modified natural zeolites	5.0	20	14.31	6
Spent activated clay	2.0	40	1.42	7
Activated alumina	4.0	25	7.44	8
Activated charcoal	2.0	40	12.87	8
Montmorillonite-supported magnetite nanoparticles	2.5	25	15.3	9
GCM nanocomposites	2.0	20	12.86	This study

Reference

1 T. W. Weber and R. K. Chakravorti, *Am. Inst. Chem. Eng*. 1974, **20**, 228.

2 J. Zhu , S. Wei, H. Gu, S. B. Rapole, Q. Wang, Z. Luo, N. Haldolaarachchige, D. P. Young and Z. Guo, *Environ. Sci. Technol*. 2012, **46 (2)**, 977.

3 Hui-Ling, M.; Youwei, Z.; Qi-Hui, H.; Dong, Y.; Zhong-Zhen, Y. and Maolin, Z, *J. Mater. Chem*. 2012, **22 (13)**, 5914.

4 H. Jabeen, V. Chandra, S. Jung, J. W. Lee, K. S. Kim and S. Bin Kim, *NANOSCALE* 2011, **3 (9)**

3583.

5 A. Dong, J. Xie, W. Wang, L. Yu, Q. Liu and Y. Yin, *J. Hazard. Mater*. 2010, **181 (1-3)**, 448.

6 Y. Zeng, H. Woo, G. Lee and J. Park, *Microporous Mesoporous Mater*. 2010, **130 (1-3)**, 83.

7 C. Weng, Y. C. Sharma and S. Chu, *J. Hazard. Mater*. 2008, **155 (1-2)**, 65.

8 S. Mor, K. Ravindra and N. R. Bishnoi, *Bioresour. Technol*. 2007, **98 (4)**, 954.

9 P. Yuan, M. Fan, D. Yang, H. He, D. Liu, A. Yuan, J. Zhu and T. Chen, *J. Hazard. Mater*. 2009, **166 (2-3)**, 821.